PERGAMON

Neural Networks 14 (2001) 657–673

Neural Networks

www.elsevier.com/locate/neunet

2001 Special issue

Propagation of cortical synfire activity: survival probability in single trials and stability in the mean

Marc-Oliver Gewaltig[a,*], Markus Diesmann[b], Ad Aertsen[c]

[a]*Future Technology Research, Honda R&D Europe (Deutschland) GmbH, 63073 Offenbach/Main, Germany*
[b]*Department of Nonlinear Dynamics, Max-Planck-Institut für Strömungsforschung, 37073 Göttingen, Germany*
[c]*Neurobiologie und Biophysik, Inst. für Biologie III, Albert-Ludwigs-Universität, Schänzlestr. 1, 79104 Freiburg, Germany*

Received 21 March 2001; accepted 26 March 2001

Abstract

The synfire hypothesis states that under appropriate conditions volleys of synchronized spikes (*pulse packets*) can propagate through the cortical network by traveling along chains of groups of cortical neurons. Here, we present results from network simulations, taking full account of the variability in pulse packet realizations. We repeatedly stimulated a synfire chain of model neurons and estimated activity (a) and temporal jitter (σ) of the spike response for each neuron group in the chain in many trials. The survival probability of the activity was assessed for each point in (a, σ)-space. The results confirm and extend our earlier predictions based on single neuron properties and a deterministic state-space analysis [Diesmann, M., Gewaltig, M.-O., & Aertsen, A. (1999). Stable propagation of synchronous spiking in cortical neural networks. *Nature*, *402*, 529–533].

Keywords: Spiking neurons; Integrate-and-fire neurons; Spike patterns; Synfire chains; Pulse packets; Cortical dynamics; Variability; Single-trial analysis

1. Introduction

According to the classical view, firing rates play a central role in neuronal coding (Barlow, 1972, 1992). The firing rate approach indeed led to fundamental insights into the neuronal mechanisms of brain function (e.g. Georgopoulos, Taira & Lukashin, 1993; Hubel & Wiesel, 1977; Newsome, Britten & Movshon, 1989). In parallel, however, a different concept was developed, according to which the temporal organization of spike discharges within functional groups of neurons, so-called neuronal assemblies (Hebb, 1949), also contribute to neural coding (Abeles, 1982a, 1991; Gerstein, Bedenbaugh & Aertsen, 1989; Palm, 1990; Singer, 1993; von der Malsburg, 1981). It was argued that the biophysics of synaptic integration favors coincident presynaptic events over asynchronous events (Abeles, 1982b; Softky & Koch, 1993). Accordingly, synchronized spikes are considered as a property of neuronal signals, which can indeed be detected and propagated by other neurons (Johannesma, Aertsen, van den Boogaard, Eggermont & Epping, 1986; Perkel & Bullock, 1968). In addition, these spike correlations must be expected to be dynamic, reflecting varying affiliations of the neurons depending on the stimulus or behavioral context. Such dynamic modulations of spike correlation at various levels of precision have in fact been observed in different cortical areas, namely visual (Eckhorn, Bauer, Jordan, Brosch, Kruse, Munk et al., 1988; Gray & Singer, 1989; for reviews see Aertsen & Arndt, 1993; Engel, König, Schillen & Singer, 1992; Roelfsema, Engel, König & Singer, 1996; Singer & Gray, 1995), auditory (Ahissar, Bergman & Vaadia, 1992; De Charms & M, 1995; Eggermont, 1992; Sakurai, 1996), somato-sensory (Nicolelis, Baccala, Lin & Chapin, 1995), motor (Murthy & Fetz, 1992; Sanes & Donoghue, 1993), and frontal (Abeles, Bergman, Margalit & Vaadia, 1993a; Abeles, Vaadia, Prut, Haalman & Slovin, 1993b; Aertsen, Vaadia, Abeles, Ahissar, Bergman, Karmon et al., 1991; Prut, Vaadia, Bergman, Haalman, Hamutal & Abeles, 1998; Vaadia, Haalman, Abeles, Bergman, Prut, Slovin et al., 1995).

Little is known, however, about the functional role of the detailed temporal organization in such signals. The first important hints towards the importance of accurate spike patterns came from the work of Abeles and colleagues (Abeles et al., 1993a,b; Prut et al., 1998). They observed that multiple single-neuron recordings from the frontal cortex of awake behaving

* Corresponding author. Tel.: +49-69-890-11-739; fax: +49-69-890-11-749.

E-mail addresses: marc-oliver.gewaltig@hre-ftr.f.rd.honda.co.jp (M.-O. Gewaltig), diesmann@chaos.gwdg.de (M. Diesmann), aertsen@biologie.uni-freiburg.de (A. Aertsen).

0893-6080/01/$ - see front matter
PII: S0893-6080(01)00070-3

monkeys contain an abundance of precise spike patterns. These patterns had a duration of up to several hundred milliseconds and repeated with a precision of ~1 ms. Moreover, these patterns occurred in systematic relation to sensory stimuli and behavioral events, indicating that these instances of precise spike timing play a functional role. In another study, Riehle and colleagues found that simultaneously recorded activities of neurons in monkey primary motor cortex exhibited context-dependent, rapid changes in the patterns of coincident action potentials during performance of a delayed-pointing task (Riehle, Grün, Diesmann & Aertsen, 1997). Accurate spike synchronization occurred in relation to external events (visual stimuli, hand movements), commonly accompanied by discharge rate modulations, however, without precise time-locking of the spikes to these external events. Accurate spike synchronization also occurred in relation to purely internal events (stimulus expectancy), where firing rate modulations were distinctly absent. These findings indicate that internally generated synchronization of individual spike discharges may subserve the cortical organization of cognitive motor processes. The clear correlation of spike coincidences with stimuli and behavioral events underlines their functional relevance (Riehle et al., 1997; see also Fetz, 1997).

Independent evidence for the possibility of precise spike timing in cortical neurons came from intracellular recordings in vitro (Mainen & Sejnowski, 1995; Nowak, Sanchez-Vives & McCormick, 1997; Stevens & Zador, 1998; Volgushev, Christakova & Singer, 1998) and in vivo (Azouz & Gray, 1999).

2. Synfire chains

On the basis of the characteristic anatomy and physiology of the cortex, Abeles (1982a, 1991) proposed that 'synfire' activity, propagating in volleys through the sparsely firing cortical neural network, presents a natural explanation for the observed precise spatio-temporal firing patterns. According to this model, the cortical network can locally be described as a sequence of groups of neurons, connected in a feed-forward way by so-called *divergent/convergent* connections, such that they form a chain-like structure. Enumerating the groups from 1 to l, we can describe the pattern of connectivity as follows: each neuron in group i receives input from a number of neurons in the preceding group $i-1$, and projects its axons to a number of neurons in the subsequent group $i+1$ (Fig. 1). The neurons within a group, however, are not mutually connected. The number of neurons per group is called the *width* w of the chain.

This architecture was first proposed by Griffith (1963) in the context of a discussion on network stability, and was called *complete transmission line*. Abeles argued that under certain conditions, Griffith's transmission line is able to reliably transmit volleys of synchronous spikes, and coined the term *synfire chain* for a structure which is able to support this mode of transmission (Abeles, 1982a, 1991).

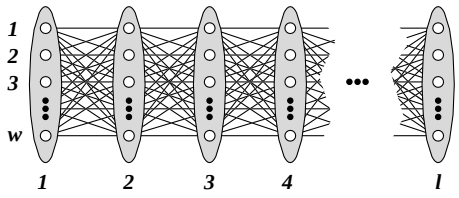

Fig. 1. Complete transmission line according to Griffith (1963). Groups (gray filled ellipses) of w neurons (white filled circles) are arranged into a feed-forward, chain-like network of length l. Neuron groups are numbered from 1 to l. The network is complete in the sense that each neuron in group $i \in \{2, \ldots, l-1\}$ receives input from all neurons in group $i-1$ and sends output to all neurons in group $i+1$ (indicated by lines). The structure is called *synfire chain* if it supports the transmission of synchronous spikes (Abeles, 1982a, 1991).

If all neurons in the first group are activated synchronously, they will cause the neurons of the second group to fire synchronously and so on. Thus, each activated group will pass a spike volley on to the next group. This process will continue, until either the chain comes to an end, or other (e.g. inhibitory) processes interfere, causing the activity propagation to stop.

Evidently, there are two possible fates of activity propagation after an initial stimulation of the first group. Either, the spike volley propagates more or less unaffected through the entire chain, or the network returns to its mode of spontaneous activity after a short lasting, stimulus-induced increase in activity. Other scenarios are unlikely, because there are neither recurrent connections, nor is there any (adaptive) inhibition that would allow for richer activity dynamics. However, we must consider that a synfire chain is embedded in the large cortical network, feeding variable background input into the chain. Here, we assume that the synfire chain is a sub-network distinguished only by the structure and not the strength of its connections. Thus, connections that define the synfire structure are identical in strength to the connections from the surrounding network. As a result of this embedding, the firing of neurons, participating in the synfire chain, will also depend on the ongoing background activity (Arieli, Sterkin, Grinvald & Aertsen, 1996b; Boven & Aertsen, 1990) and will, thus, be quite variable.

For activity propagation in such a synfire chain, the following problems are immediately obvious.

First, even if all neurons in the first group fire in synchrony, the neurons in the second group will generally not. There will always be some temporal jitter in their firing times, due to the uncorrelated background input. In an optimal case, this jitter will not build up, resulting in a stationary accuracy which remains in the few-millisecond range. However, it is also possible that the jitter does build up at each stage, causing the synfire to cease after passing only a few groups.

Second, spontaneous activity may either cause some neurons in a group to be refractory when the input volley arrives or hyper-polarize their membrane potential. These

neurons will then be unable to contribute their share to the activation of the next group. Hence, the number of spikes in the second group may be smaller than the initial number of spikes. Again, this effect may build up, finally causing propagation to fail. Alternatively, it may reach an equilibrium, which still allows further propagation. The idea behind the synfire chain is that the firing probability of a neuron is much higher if it receives its input spikes in a synchronous fashion. Since the contribution of each presynaptic neuron is relatively small, the system may still work, even if a small enough number of neurons in a group fails to participate.

Thus, with respect to the electrophysiological properties of cortical neurons, the synfire hypothesis raises the following questions.

1. Is the transmission line able to propagate synchronous spike activity, given the properties of cortical neurons, and what are the neuronal and network constraints?
2. Is the achieved accuracy of synfire activity consistent with the precision of experimentally observed firing patterns (~1 ms)?
3. Can the accuracy of synfire activity be maintained long enough to explain the duration of the observed precise spike patterns (up to several hundred milliseconds)?
4. How robust is the synfire mode of activity propagation to perturbation?

It is useful to regard a spike volley which *propagates* along a synfire chain as an entity. We call this entity a *pulse packet* (Aertsen, Diesmann & Gewaltig, 1996; Diesmann, Gewaltig & Aertsen, 1996; Gewaltig, Diesmann & Aertsen, 1995). In simulation studies of a physiologically realistic model (Diesmann, Gewaltig & Aertsen, 1999), we could provide an answer to the first two questions. There, we used the notion of *pulse packets* to describe the propagation of short-lasting volleys of synchronized spiking activity. Such pulse packets were characterized by two parameters: the number of spikes a in the volley and their temporal spread σ. Thus, a novel transmission function, describing probability and temporal spread of response spikes to pulse packet input, was computed. Interpreting a and σ as deterministic state variables, we could predict the propagation of synchronous activity in a synfire chain network on the basis of the transmission function. Practically identical results were obtained for a reduced integrate-and-fire model, demonstrating that these findings present generic properties of integrate-and-fire dynamics (Diesmann, Gewaltig & Aertsen, 2001). From these results, we conclude that a chain, consisting of some 100 neurons per group is structurally strong enough to support stable propagation of spiking activity along the chain (Question 1). Moreover, our results indicate that the spiking precision of the stably propagating pulse packet is consistent with the precision of the experimentally observed firing patterns (Question 2). The purpose of the present study is twofold. First, we want to make a contribution towards answering Questions 3 and 4. Second, we want to investigate whether the results from our two-dimensional state space analysis can be confirmed in network simulations, taking full account of the variability in individual pulse packet realizations. In our previous paper, we described the *dynamics of the mean* behavior of pulse packet transmission. At each point in the a–σ space, we determined the expected transformation of the pulse packet. Here, we focus on the dynamics of propagating pulse packets in individual realizations. We trace the propagation of a pulse packet through the entire synfire network over repeated trials. Thus, we will be able to assess the survival probability of pulse packet transmission in individual trials. Preliminary results were published in abstract form (Gewaltig, Diesmann & Aertsen, 2001).

3. Model neuron

For our simulation studies, we used an *integrate-and-fire* type model neuron (Lapicque, 1907; Tuckwell, 1988). An earlier version of this model was described by Gewaltig, Diesmann, Aertsen and Abeles (1994).

3.1. Membrane properties

The membrane potential of the neuron $U(t)$ is the main state variable, described by the differential equation (1):

$$C\frac{\mathrm{d}}{\mathrm{d}t}U + \underbrace{\sum_{i\in p} g_i(U-E_i)}_{\text{passive}} + \underbrace{\sum_{i\in a} g_i(t)(U-E_i)}_{\text{active}} = I(t). \qquad (1)$$

The membrane potential is influenced by various types of currents. Among them are active and passive ionic currents, as well as synaptic and external currents. Only the ionic currents are assumed to depend on the membrane potential $U(t)$.

3.2. Spike generation

A threshold Θ, combined with an absolute refractory mechanism, is responsible for the generation of action potentials. The refractory mechanism prevents the generation of a second spike for a given period of time t_r after the membrane potential has crossed the threshold Θ and elicited a spike.

The active ionic currents (Na^+, slow and fast K^+) model the shape of the action potential as well as the subsequent after-hyperpolarization (AHP) (e.g. Kandel, Schwartz & Jessel, 1991). They are started by the spike generation mechanism and have the form

$$I_i(t) = g_i(t)(U(t) - E_i) \qquad (2)$$

for each of the channel species Na^+, K^+_{fast}, K^+_{slow}. Here, E_i is the reversal potential and $g_i(t)$ the conductivity for the specific ionic current.

The conductivities are all modeled by a double

Table 1
Parameters of ionic currents

	Na^+	K^+, fast	K^+, slow
Reversal potential (mV)	45.0	−75.0	−75.0
Peak value (μS)	5.0	2.0	0.017
Time to maximum (ms)	0.1	1.0	1.0
Decay time constant (ms)	0.3	3.0	20.0

exponential function $g(t)$:

$$g(t) = g_0 \cdot (e^{-t/\tau_1} - e^{-t/\tau_2}) \cdot H(t), \tag{3}$$

with $H(t)$ the unit-step function:

$$H(t) := \begin{cases} 1, & t \geq 0; \\ 0, & t < 0. \end{cases} \tag{4}$$

Choosing $\tau_1 > \tau_2 > 0$ ensures that $g(t)$ is positive for all $t > 0$.

The sodium current is responsible for the steep rising phase of the action potential (AP). The fast potassium current helps in rapidly returning the membrane potential back to its resting value. Finally, the slow potassium current generates a long lasting AHP. Table 1 summarizes the various parameters of the active ionic currents.

3.3. Linear membrane properties

The ionic currents decay fast and can be neglected after a certain period of time following an action potential. Eq. (1) can then be approximated by a linear differential equation with constant coefficients:

$$C \frac{\mathrm{d}}{\mathrm{d}t} U + \sum_{i \in p} g_i (U - E_i) = I(t). \tag{5}$$

This can be rewritten in the familiar form of the so-called *leaky integrator* equation:

$$\frac{\mathrm{d}}{\mathrm{d}t} U + \frac{1}{\tau} U = \frac{1}{C} I'(t), \tag{6}$$

with $\tau := C / \sum g_i$ and $I'(t) := I_{\mathrm{rest}} + I(t)$, where $I_{\mathrm{rest}} := \sum g_i E_i / C$. The constant current I_{rest} maintains the resting potential of the membrane. The constant τ is usually called *membrane time constant*.

The various parameters of the model are summarized in Table 2. They were chosen to conform to the experimental literature (Kandel et al., 1991; Tuckwell, 1988) and resulted in a value of the membrane time constant of $\tau = 10$ ms.

3.4. Post-synaptic currents

Post-synaptic currents (PSC) are modeled by alpha functions (e.g. Jack, Noble & Tsien, 1985; Tuckwell, 1988):

$$I_{\mathrm{syn}}(t) = \alpha_0 \cdot t \cdot e^{-t/\tau_\alpha} \cdot H(t). \tag{7}$$

Here, α_0 determines the peak amplitude and τ_α denotes both the time to peak and the decay time constant of the PSC.

Table 2
Membrane parameters

Parameter	Value
Capacitance C (pF)	250
Membrane time constant τ (ms)	10
Threshold Θ (mV)	−55
Mean distance to threshold (mV)	7.3
Refractory period (ms)	1

A post-synaptic potential (PSP) is the perturbation of the membrane potential, caused by a single incoming PSC. Assuming that all active ionic currents are negligible and the membrane is essentially linear, we can solve Eq. (6) for a single PSC:

$$U_{\mathrm{psp}} = \frac{\alpha_0 \cdot \Delta^2}{C} \left(e^{-t/\tau} - e^{-t/\tau_\alpha} \cdot \left(1 + \frac{t}{\Delta} \right) \right) \cdot H(t) \tag{8}$$

with $1/\Delta := 1/\tau_\alpha - 1/\tau$ and τ the membrane time constant. Note that $\tau_\alpha \ll \tau$. Moreover, it is important to note that the properties of the initial phase of the PSP are governed by the PSC, while membrane properties determine the falling phase of the PSP. The constants α_0 and τ_α were chosen to yield physiologically realistic values for the PSP amplitude (0.14 mV), rise time (1.7 ms), and half width (8.5 ms) (Fetz, Toyama & Smith, 1991).

3.5. Synaptic background activity

It has long ago been suggested that the large fluctuations of the membrane potential, exhibited by neurons under in vivo conditions, can be accounted for by the varying number of synaptic events impinging on a neuron at any time (Calvin & Stevens, 1968). Presumably, these fluctuations are to a large extent response for the so-called *spontaneous activity* of a neuron, that is, the occurrence of spike events in the absence of a (controlled) stimulus.

Anatomical data suggest that a cortical pyramidal cell has on the order of 10^4 synapses (Braitenberg & Schüz, 1991). These include synapses from excitatory and inhibitory neurons. One can estimate the net effect of these synapses on the neuron by assuming randomly (Poissonian) arriving events at each of the synapses. Assuming stationarity, constant rates λ_e and λ_i can be assigned to the excitatory and the inhibitory events, respectively.

Estimates for all these parameters can be found in the electrophysiological and anatomical literature (e.g. Abeles, 1991; Braitenberg & Schüz, 1991; Fetz et al., 1991). In most cases, the estimates leave enough room to allow for some adjustment of the model. Here, the rates λ_e and λ_i were chosen such that the resulting spontaneous activity of the model neuron is consistent with the assumed excitatory input rate λ_e. Therefore, we can simulate the embedding of our sub-network simply by supplying each neuron with independent excitatory and inhibitory Poisson sources of

Table 3
Parameters of synaptic background activity

	Excitatory	Inhibitory
Percent of all synapses	88	12
Mean firing rate (Hz)	2.00	12.54
PSC amplitude (pA)	45.63	−45.63
PSP amplitude (mV)	0.14	−0.14
PSP rise time (ms)	1.7	1.7

these rates. The parameters used for the model neuron are summarized in Table 3.

4. Network structure

4.1. Width of a synfire chain

Within the cortical network, the structural parameters of a synfire chain are governed by various anatomical and physiological constraints, such as the proximity of the participating neurons (Hehl, Hellwig, Rotter, Diesmann & Aertsen, 2001) and the characteristics of the inhibitory circuitry. However, this information is not easily accessible.

We can estimate the minimal width w of a synfire group by considering the number of synchronous spikes, a_s, needed to bring the membrane potential to the firing threshold Θ:

$$a_s = \frac{\Theta - U_{rest}}{psp_0} \tag{9}$$

$$= \frac{7.3\ mV}{0.14\ mV} \approx 52. \tag{10}$$

Assuming a symmetric membrane potential distribution and neglecting the temporal extent of a post-synaptic potential, an input of a_s synchronous spikes yields a response spike with 50% probability. However, to ensure stable propagation, it is necessary that the number of response spikes $\hat{a}$ at each neuron group at least matches the number of input spikes a_s:

$$\hat{a} \geq a_s. \tag{11}$$

The expected number of output spikes is given by the product of the response probability of a single neuron and the number of available neurons, w. Thus:

$$\frac{1}{2} \cdot w \geq a_s \tag{12}$$

$$\Rightarrow w \geq 2 \cdot a_s \approx 104. \tag{13}$$

Since the post-synaptic potential has finite rise- and decay-times, the response probability for a_s input spikes will, in fact, be larger than 50%. It turns out that a group size of about $w = 100$ neurons is sufficient to support stable propagation (see also Diesmann et al., 1999).

4.2. Delay between groups

The transmission delay is the time needed for a spike to travel from one neuron to the next. In our model, it combines the axonal delay, the synaptic delay, as well as the dendritic delay. More important than the absolute value of the transmission delay is the question whether its values are uniform across all connections between two groups, or whether they scatter according to some distribution. If the delays are identical for all connections, their value merely sets the lower limit on the minimal spike interval in a spatio-temporal firing pattern. However, if the delays follow some distribution, this delay distribution will effectively limit the maximal precision of firing patterns (see also Wennekers & Palm, 1996).

Assuming that a synfire chain is the result of an active learning process which encourages synchrony by means of some temporal learning rule (e.g. Bi & Poo, 1998; Gerstner, Kempter, van Hemmen & Wagner, 1996; Gütig, Aharonov-Barki, Rotter, Aertsen & Sompolinsky, 2001; Markram, Lübke, Frotscher & Sakmann, 1997; Rubin, Lee & Sompolinsky, 2001; Song, Miller & Abbot, 2000), it is conceivable that all delays between neurons in successive groups are approximately the same. Thus, we assume a uniform delay of 1 ms between neurons in adjacent groups.

4.3. Length of a synfire chain

The length l of the synfire chain determines the number of successive groups. Thus, it imposes an upper limit on the duration of a spatio-temporal pattern, provided the chain does not entail recurrent connections (see, e.g. Abeles et al., 1993a). The length of the chain limits the amount of time available for the activity dynamics but, apart from this, it has no critical influence on the stability of activity propagation. Thus, in our simulations, l must be chosen such that we can observe the system for a sufficient period of time to fully capture the dynamics of activity propagation, and to distinguish between the two modes of activity: survival or termination of synchronous spiking activity. Here, we chose $l = 20$.

5. Experimental procedure

Activity propagation in a synfire chain can be triggered, using a stimulus which mimics the output of a more or less synchronous group of input neurons, sending activity into the chain. Thus, the first group receives input in the form of artificially generated pulse packets, each consisting of a_0 spike times drawn from a Gaussian distribution with standard deviation σ_0. We then investigate how this pulse packet propagates along the model synfire chain, depending on the stimulus parameters (i.e. a_0 and σ_0).

Since the behavior of the chain will not be exactly the same in different repetitions of the experiment, due to the fluctuating background activity, we will perform multiple trials for each choice of stimulus parameters.

Since each neuron responds to an input pulse packet with at most one spike, the upper limit of the number of response spikes from a group is given by the group width w (here $w = 100$). Obviously, the lower limit is 0. The lower limit of

the temporal dispersion is 0 ms in the limit of a fully synchronized spike volley. For the upper value of σ_0, we determined the largest value of σ_0 which is still able to elicit propagating synfire activity. This resulted in a value around 5 ms, consistent with our earlier single neuron study (Diesmann et al., 1999).

The parameter space is, thus, given by the Cartesian product of these two parameter ranges:

$$\mathbf{R}_{\sigma_0} := [0\text{ ms},\ 5\text{ ms}], \tag{14}$$

$$\mathbf{R}_{a_0} := [0,\ 100], \tag{15}$$

$$\mathbf{R}_{(a_0,\sigma_0)} := \mathbf{R}_{a_0} \times \mathbf{R}_{\sigma_0}. \tag{16}$$

The stimulation parameters are chosen such that they cover the borders of the parameter space. That is, one set of parameters is chosen by setting the activity $a_0 = 100$, while varying the value of the dispersion σ_0 between 0 and 5 ms. Another set is chosen by setting $\sigma_0 = 0$, while varying the value of a_0 between 0 and 100 spikes. The model computations are performed with a simulation step size of $h = 0.1$ ms. Before any stimulus is applied, the random number generator is initialized and the network is simulated for a period of 500 ms. This ensures that initial transients have vanished, and that the network activity has reached an equilibrium state of low spontaneous activity (≈ 2 spikes/s). For each parameter configuration, 50 trials are performed. In each trial, a new stimulus packet is generated. This stimulus is applied to the neurons of the first group and the response of all neurons in the chain is measured. After the stimulus has been applied, the simulation continues for a period of time which is sufficiently long to allow any induced activity to propagate through the entire length of the chain.

Each trial is followed by a simulation period of 250 ms without stimulation, to ensure that the network can relax to its equilibrium state of low spontaneous firing. After this period, either the next trial starts, or a new choice of parameters is used.

6. Propagating synfire activity

6.1. Overview

Fig. 2 shows four typical raster displays of propagating synfire activity. The panels in this and all subsequent figures are arranged such that the stimulus activity a_0 increases from bottom to top, and the stimulus jitter σ_0 increases from left to right. Panels A and C show cases where the chain was started with different numbers of fully synchronized input spikes. The spike volley in A is able to build up enough activity to propagate along the entire chain. The temporal spread initially builds up, but remains stationary at a certain level. By contrast, C shows a case where the dispersion of the spikes increases at each group, and activity propagation ceases before the end of the chain is reached. Panels B and D illustrate the response of the same network to a large number of differently distributed input spikes. Panel B demonstrates that the system is able to reduce an initial jitter to some residual amount. By contrast, in D, activity propagation does not reach the end of the chain. Here, the number of spikes in a volley steadily reduces from group to group, despite the decrease in temporal spread. Finally, the group activity becomes indistinguishable from the background activity.

Overall, we observed four distinct modes (A–D) of activity propagation with two different *fates*. Either the initial stimulus was strong and/or concise enough to assure stable propagation of synchronous activity (A and B), or it was not (C and D). In the latter case, the activity propagation ceases after only a few groups. Each neuron contributes at most one spike to a group response, and, although the input to the neurons is quite strong, we do not observe bursts of spikes. In the following sections we will present a conceptual framework to describe the diversity of the observed propagation dynamics.

6.2. Pulse packet propagation in time

For a more quantitative investigation of the activity propagation, we return to the characteristic measures of a pulse packet: the number of spikes it contains, a, their temporal dispersion, σ, and the center of gravity of the pulse packet, $\langle t \rangle$, reflecting the average response spike time. The pulse packet itself consists of the set of a response spike times of a synfire group: $\mathrm{pp} = \{t_1 \le t_2 \le \cdots \le t_a\}$. The number of events a is called the *activity* of the packet. For each trial, the pulse packet properties for each neuron group are estimated from the recorded spike data, using the formulae:

$$\langle t \rangle := \frac{1}{a} \sum_{j=1}^{a} t_j \tag{17}$$

$$\sigma^2 := \frac{1}{a} \sum_{j=1}^{a} (\langle t \rangle - t_j)^2. \tag{18}$$

The actual estimation and the separation of the pulse packet from the ongoing activity are described in the Appendix.

To trace the activity propagation along the synfire chain, we evaluated the series of estimated values of a_i, σ_i at each group i of the chain for each of the 50 repeated trials.

Fig. 3 shows the activity a of the group response versus the group index, that is, the number of response spikes of that particular group for the same input pulse packets as in Fig. 2. Knowing that the propagating pulse packet activates the individual groups one after the other, the graphs can be interpreted as describing the evolution of the activity as the pulse packet propagates along the synfire chain. Note the incomplete curves of the unsuccessful trials (panels C and D), and the large variability between different trials.

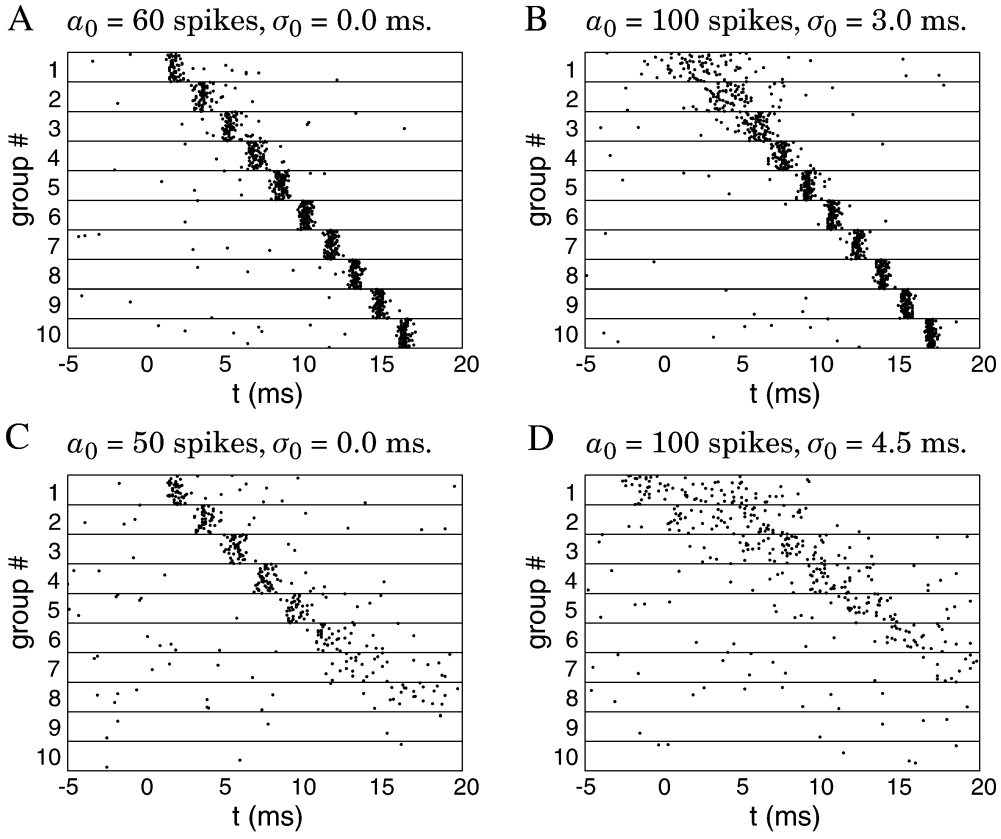

Fig. 2. Four characteristic raster displays of evoked synfire activity. Stimulus parameters (a_0, σ_0) are specified in panel titles. The stimulus packet (not shown) with a_0 spikes is drawn from a Gaussian spike time distribution of standard deviation σ_0, centered at time 0. Network structure is $w = 100$, $l = 20$ (cf. Fig. 1) with a synaptic delay of 1 ms. Neuron model and the model of background activity are described in the text and are used consistently throughout the paper. Each row in a panel shows the spiking activity of a synfire group versus time (first 10 groups shown). The top row refers to the first group in the synfire chain, lower ones refer to later groups. Within each row, a unique vertical position is reserved for the spikes of a particular neuron. Spike events are marked by dots. The panels are arranged such that the dispersion σ_0 of the stimulus volley increases from left to right and the activity a_0 of the stimulus increases from bottom to top. (A) Low initial activity with high synchronization. Activity increases gradually, and is able to propagate along the entire length of the chain. Temporal dispersion increases before the volley resynchronizes and stabilizes at some residual spread. (B) High initial activity with moderate synchronization. The spike volley gradually synchronizes its activity, finally reaching stable transmission. Activity of the volley is minimal around group number 2. (C) Similar conditions as in A, with fewer spikes. In this case, the spike volley is not able to gain enough activity to survive. The packet gradually disperses and in later groups rapidly loses spikes. The network returns to its spontaneous firing mode. (D) Similar initial conditions as in B, but slightly larger dispersion. Initially the spike volley synchronizes and reaches a minimal spread at groups 4 and 5. A steady loss in activity eventually causes the propagation to fail. Once the packet stabilizes, the observed delay between successive group activations is about 1.5 ms in panels A and B. In A, the last group is activated at $t = 16$ ms, and at $t = 17$ ms in B. In C, the delay between group activations is about 1.8 ms, and 2.5 ms in D. The sixth group in D is activated only after some 16 ms.

Panels A and C represent cases with low initial activity at a high degree of synchronization. In A, the activity curves increase monotonically, until they saturate after some 10 groups at a value of about 90% of the available neurons. Note that in all trials, the activity survives until the end of the chain and stays close to the trial average (gray). By contrast, in C, 52% of the traces decrease, until the activity is no longer measurable. In these cases, the pulse packet propagation did not reach the end of the chain. Observe that in a number of cases, the activity remains approximately constant over some groups. However, if the activity goes below a certain 'threshold', it rapidly decreases. Moreover, in C, the variability between trials is larger than in A. For those trajectories which do eventually saturate, the variability is largest between groups 5 and 10.

Panels B and D show the opposite case with high initial activity and moderate to low synchronization. In B, the activity curves are non-monotonic. They first reach a pronounced minimum, until they again saturate at about 90 spikes. As in A, the variability between trials is low. While in B, the pulse packet survives in all trials, this is clearly different in D. Here, 58% of the curves decrease monotonically and terminate before the end of the chain. The remaining traces saturate at a high activity value after their minimum at group 2. Moreover, the variability is larger than in B.

For all four initial conditions, we observe convergence of the surviving activity curves towards the same asymptotic value. Moreover, the activity converges quite fast. After only about 10 groups, the asymptotic value is reached. This activity value appears to be independent of the initial conditions. However, the initial value does influence if and how the

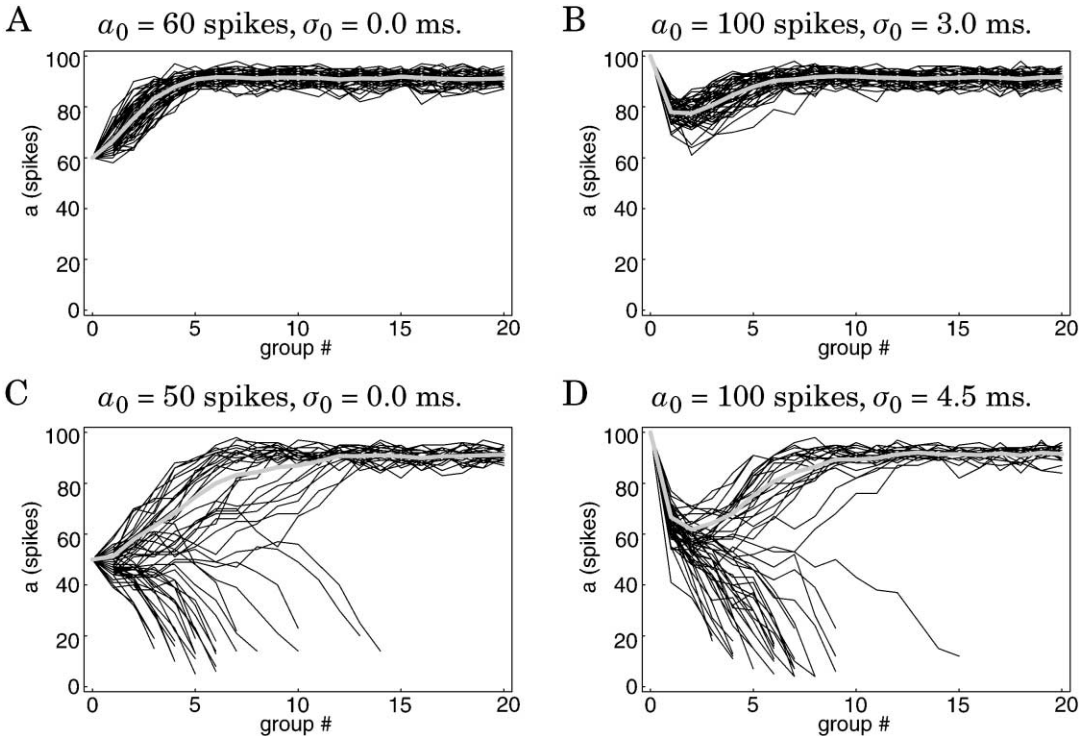

Fig. 3. Evolution of pulse packet activity a versus group index for four different initial conditions (arrangement of panels and parameters identical to Fig. 2). The stimulus (specified in panel title) is included at group number 0. Each panel shows the result of 50 repetitions of the simulation with identical stimulus parameters. Measurements from successive groups are connected by lines for better readability. Black lines correspond to individual trials, gray lines are trial averages of the surviving trials. Unsuccessful trials are distinguished by activity which vanishes before the end of the chain is reached (lines terminating at a group # $<$20). In panels (A) and (B) activity stabilizes at $a = 90$ in 100% of the trials. In (C), 48% and in (D) 42% of the trials reach the end of the chain. Variability between different trials is large, especially in the transient regime where trials separate between success and failure. The general development of the activity of the majority of the trials in each panel is different in all four cases. The successful trials in C (minority) develop similar to the activity in A, successful trials in D (minority) similar to the activity in B.

asymptotic value is reached. After some five groups, surviving and decaying cases can be separated. During the transient phase (in particular in C and D), variability between trials is large. However, once the asymptotic value is reached, it is very low. As a consequence, two identical synfire chains, even when ignited simultaneously with an identical stimulus, may still evolve quite differently in time.

Fig. 4 shows the standard deviation of the response spike times, i.e. their temporal jitter σ, versus the group index for the same initial conditions as in Fig. 3. Compared to the activity plots, monotony is reversed. We observe non-monotonic behavior of the successful trials in Fig. 4, where we observed monotonic behavior in Fig. 3, and vice versa.

Panels A and C represent cases of low initial activity and a high degree of synchronization. In A, the dispersion initially increases, before it falls again to some residual jitter below 0.5 ms, indicating a high degree of synchrony of the propagating response spikes. The successful trials in C show the same qualitative behavior. By contrast, in C, the response dispersion of the unsuccessful trials shows a continuous increase, until the propagation terminates.

Panels B and D show cases with high initial activity and moderate to low synchronization. In B, the dispersion of the propagating pulse packet falls monotonically, until it again relaxes to a value below 0.5 ms. By contrast, the unsuccessful trials in D, even though initially decreasing in temporal spread, rapidly increase again, until they terminate at a value of σ above 1 ms.

We can observe some common features in the behavior of the pulse packet activity a and its dispersion σ. Both response characteristics develop from their initial values towards an asymptotic value, which is independent of the initial conditions. Moreover, this relaxation is fast. After only 10 groups, dispersion and activity of the propagating pulse packet remain approximately constant. During the initial groups, however, we observe considerable variability between individual trials which, for the successful trials, reduces towards the end of the chain.

6.3. State space for pulse packets

Activity a and dispersion σ describe different aspects of the propagating pulse packet. In analogy to the stimulus parameters, we combine the response characteristics to a pair $(a, \sigma)_i$ to describe the *state* of the propagating pulse packet at each group i. The state of the pulse packet can then

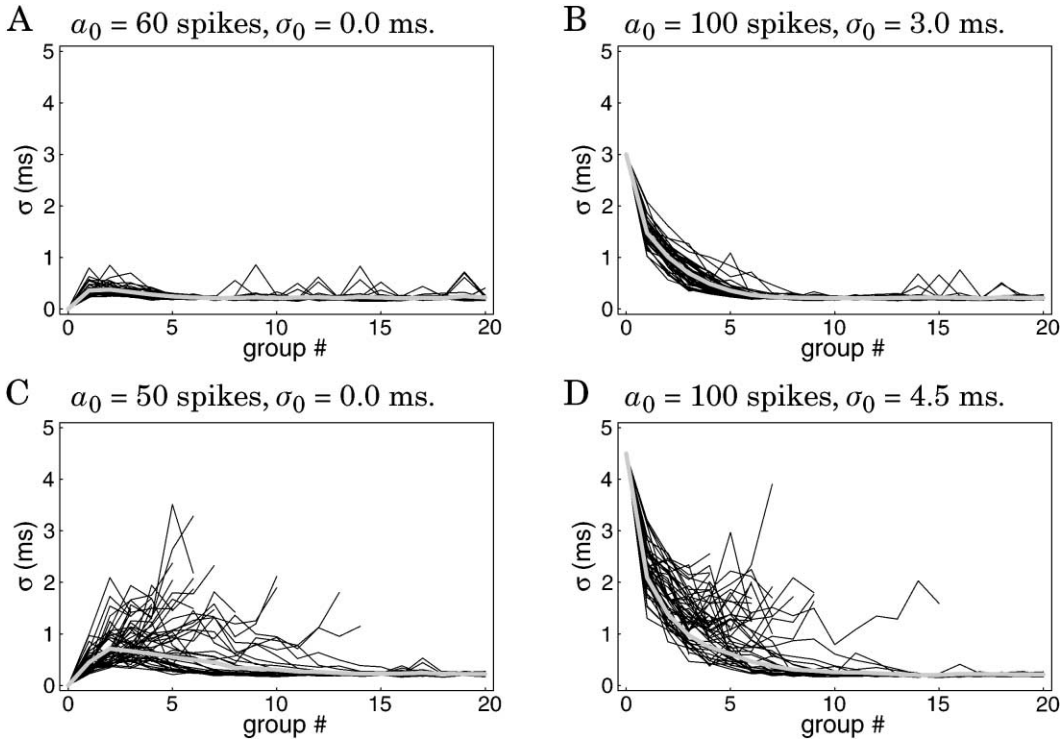

Fig. 4. Temporal dispersion σ of the pulse packet versus group index for four different initial conditions (arrangement of panels and parameters identical to Fig. 2). Same data set as in Fig. 3. Here, the σ-component is displayed instead of the a component. Graphs are constructed as in Fig. 3. Unsuccessful trials are distinguished by activity which vanishes before the end of the chain is reached (lines terminating at a group # <20). In panels (A) and (B), temporal spread stabilizes at $\sigma = 0.3$ ms in 100% of the trials. Consistent with Fig. 3 (same data) the end of the chain is reached in 48% of the trials in (C) and 42% of the trials in (D). Here, variability between different trials is large, especially in the transient regime where trials separate between success and failure. The general development of temporal spread of the majority of the trials in each panel is different in all four cases. The successful trials in C (minority) develop similar to the σ in A, successful trials in D (minority) similar to the σ in B.

be expressed as a single point in the two-dimensional a, σ space.

Fig. 5 illustrates the (a, σ) response of the first eight groups of the chain for a propagating pulse packet. Panel A shows a chain which was repeatedly activated with a pulse packet consisting of 50 fully synchronized spikes (cf. panel C in Figs. 2–4). In the first group, the responses form a rather compact cloud near the initial value. The size of this cloud is a measure of the variability between different trials. If we 'trace' this cloud from one group to the next, we observe that its size increases. This corresponds to an increase in inter-trial variability. At the same time, the total number of dots decreases from the fourth group on. This reflects the fact that at a later stage, the response packet did not survive in a fraction of the trials. The cloud broadens vertically while 'drifting' to the right. Points moving upwards correspond to successful trials, where the pulse packet was able to propagate along the entire chain. Further along the chain, they cluster in the top left corner of the state space. Points moving downwards also drift to the right, which reflects an increase in response dispersion. These points correspond to the unsuccessful trials and eventually disappear from the graph.

Panel B shows a case where the initial pulse packet was strong enough to successfully propagate through the chain in all 50 trials. Thus, we obtain a group response in every trial. Starting at the first group, we again observe that the responses form a compact cluster in the state space. In contrast to A, however, the cluster does not disperse, but becomes more and more compact as we go from one group to the next. This corresponds to a successive reduction in inter-trial variability of the group responses. Moreover, the response cloud drifts from a point near the initial value of the stimulus pulse packet to a position near the top left corner of the state space.

We obtain a more concise description of the synfire activity by interpreting the sequence of response pairs

$$\{(a, \sigma)_0, (a, \sigma)_1, \ldots, (a, \sigma)_l\},$$

for each trial as a 'trajectory' in the state space. Such a trajectory traces the state of the spike volley as it propagates from one group to the next.

Fig. 6 shows the state space trajectories for the same four initial conditions as in Fig. 2. Panel A shows the case with 60 fully synchronized spikes. All trajectories start at the same point in the state space, and remain so close together that they form an almost continuous band. The width of the band can be interpreted as a measure for the inter-trial

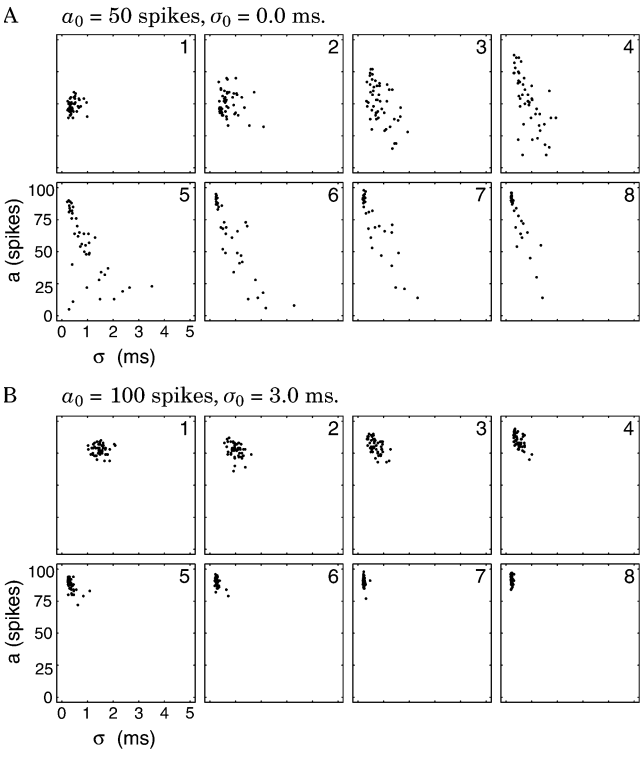

Fig. 5. (a, σ) response of the first eight groups of a chain for a propagating pulse packet. Each box represents the a–σ space (a vertical, σ horizontal) for a particular group (number in upper right corner). The sequence of eight boxes (from left to right and top to bottom) describes the development of the spike volley. Each dot marks the (a, σ) response in one of the 50 trials with identical initial conditions (specified in panel title). (A) Low initial activity at high synchronization (same data as in Figs. 3C and 4C). In 48% of the trials, the packet stabilizes at a high activity level and low temporal dispersion (upper left corner of a–σ space). In the majority of the trials, activity decays (dots move downwards), temporal spread increases (dots move to the right), and variability between trials increases (cloud of dots expands). From the fourth group on, the fraction of trials showing synchronous activity decreases (total number of dots decreases). (B) High initial activity at moderate synchronization (same data as in Figs. 3B and 4B). In 100% of the trials, activity stabilizes at a high activity level and low temporal dispersion. In the last two groups shown (7, 8) variability between trials observable in early groups (1, 4) is considerably reduced (cloud of dots shrinks).

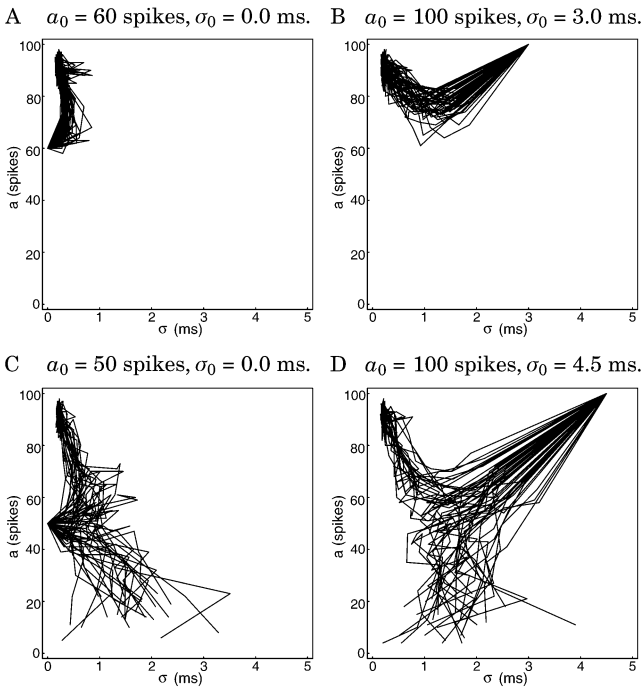

Fig. 6. State space trajectories for four different initial conditions (arrangement of panels and parameters identical to Fig. 2). Same data as in Figs. 3 and 4. (a, σ) coordinates of pulse packets in consecutive groups are connected by lines to visualize the trajectory in state space. Within each panel, the trajectories of all 50 trials are superimposed. The individual features of the development of a (Fig. 3) and σ (Fig. 4) are combined to a two-dimensional representation. Comparison of the four panels (in particular C and D) indicates that the four characteristic types of trajectories (cf. Fig. 2) are induced by the existence of an attractor at a temporal spread of 0.3 ms and activity about 90 spikes and a saddle point at a temporal spread of about 1.2 ms and activity slightly above 50 spikes. Large variability of σ can be observed at low values of a.

variability of the trajectories. All trajectories terminate around the same final point, which corresponds to a pulse packet with dispersion below 0.5 ms and activity around 90 spikes. Note that between start and end points, the trajectories are curved, indicating a non-monotonic development of the response dispersion. Moreover, variability is largest close to the starting point, and becomes considerably smaller towards the terminating point.

Panel B shows the trajectories for a stimulus with moderate initial synchronization and high activity. Again, all trajectories move away from the initial point and terminate at the same final point as in A. In the terminology of dynamical systems, this terminal point can be called an *attractor*, since it 'attracts' all trajectories in its vicinity. This time, the curvature of the trajectories indicates a non-monotonic behavior of the activity a, while the response dispersion decreases monotonically.

By contrast, C and D show cases where only part of the trajectories terminate at the attractor, whereas the majority terminates in the lower third of the state space. Note that the variability of those trajectories that do not reach the attractor is considerably larger than that of the trajectories that do. There are indications for an attractor at zero activity and finite response dispersion. However, in this region the variability in σ is too large for a reliable conclusion.

Fig. 6A–D clearly illustrates the four modes of activity propagation, discussed in connection to Fig. 2. In all four panels, Fig. 6A–D, the trajectories approach the attractor for stable pulse packet propagation along a line that runs from the lower left to the upper right of the state space. Panels C and D indicate that there exists a sharp border that separates a region in the state space from where all trajectories can reach the attractor, the *basin of attraction*, and a region from where the stable state cannot be reached. The attractor and a *saddle point* at a temporal spread of about 1.2 ms and activity slightly above 50 spikes induce the four characteristic types of trajectories.

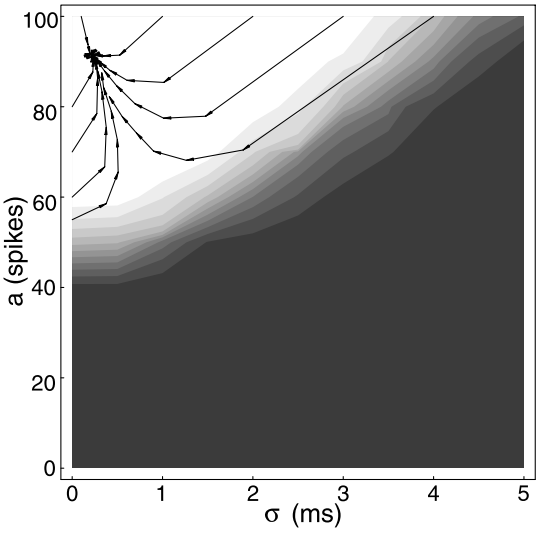

Fig. 7. State space portrait of synfire activity. The contour plot shows the survival probability of synfire activity as a function of position in state space. Light gray corresponds to high values, dark gray to low values (contour levels in steps of 10%). The trajectories show trial averages for which the packet survived in at least 50% of all trials. For a wide range of initial conditions, the pulse packet evolves towards a single attractor at high activity and low temporal spread. Within this region, all trajectories lead towards the attractor. The temporal dispersion at the attractor is well below 1 ms. The steep decline in survival probability marks the separatrix, below which all synchronous activity is probable to decay.

6.4. Survival probability

We can obtain an even more concise view of the synfire dynamics by replacing the individual trajectories for all trials by their trial average. Here, we do this only for those trajectories that eventually reach the attractor. In this case, good estimates can be obtained simply by independently averaging a and σ over all trajectories. Thus, for a given initial value, we compute the trial average only if at least 50% of all trajectories reach the attractor (Fig. 7).

A complementary approach that highlights the non-deterministic nature of pulse packet propagation is to determine the *survival probability* of a trajectory at each point in the state space. To this end, we compute how many of the trajectories, crossing a small area around that point, will eventually reach the attractor. Assuming that the mapping of (a, σ) is sufficiently smooth, we interpolated the trajectories by adding n evenly spaced sampling points along each segment of a trajectory (here $n = 7$). The survival probability was then estimated using a two-dimensional histogram with bin-size $(\Delta a = 10) \times (\Delta\sigma = 0.5$ ms). In doing so, we assume that two pulse packets with the same (a, σ) configuration are identical with respect to their survival probability. It turns out that the parameter set described in Section 5 is sufficient to reveal the survival probability in the state space.

Fig. 7 shows in gray code the survival probability of trajectories in the (a, σ)-space (light gray: high values, dark gray: low values). Superimposed are the average trajectories for different initial conditions. Each trajectory represents the path in the state space, taken on average by a propagating pulse packet.

Observe that there is a wide range of stimulus parameters for which the pulse packet evolves towards the attractor. Moreover, as discussed above, all trajectories approach the attractor in a similarly curved way. Note that once a pulse packet has reached the attractor, its state is very robust. Small perturbations will move the pulse packet to one of the neighboring trajectories, leading back into the attractor. In terms of the state variables a and σ this means that, if a pulse packet is temporarily moved away from the attractor, it is able to regain activity and to resynchronize.

In the deterministic case, the region in which the system will return to the attractor is called the *basin of attraction*, here it is distinguished by a survival probability close to 1 (white region in the figure). Note that the temporal jitter at the fixed point is well below 1 ms. This value is consistent with the precision of cortical timing, observed in both in vitro and in vivo studies, and clearly below the value of the membrane time constant (≈ 10 ms). We will return to this point in the discussion.

Observe that the border of the basin of attraction is distinguished by a steep transition of the survival probability from one (white region) to zero (black region). In the black domain, no trajectory is able to reach the attractor. At 52 fully synchronized input spikes, the survival probability is approximately 0.5. This is consistent with our previous estimation of a_s (cf. Section 4.1 Eq. (10)).

6.5. Propagation speed

So far, we neglected the temporal aspects of pulse packet propagation. We only investigated the number of response spikes and their temporal jitter, neglecting the speed of propagation.

The propagation speed v of a pulse packet can be defined as the inverse of the time needed for group i to activate the successive group $i + 1$. It can be estimated from the sequence of values of $\{\langle t\rangle_i | i = 1 \ldots l\}$ at successive groups,

$$v_i := \frac{(i+1) - i}{\langle t\rangle_{i+1} - \langle t\rangle_i}, \quad \langle t\rangle_0 = 0 \text{ ms}, \quad i = 0 \ldots (l-1). \tag{19}$$

Fig. 8 shows $\langle t\rangle_i$ versus the group index i (panels A and C) and the propagation speed v_i, measured in groups per ms, versus the group index i (panels B and D). As in Fig. 3, black lines represent individual trials, gray curves represent trial averages for the surviving trials.

In A, the development of $\langle t\rangle_i$ is almost linear, with very little variability between trials. However, in B, we observe a slight initial increase in the speed of the propagating pulse, but it quickly saturates at a constant value, slightly above 0.6 groups/ms.

In C, the traces of $\langle t\rangle_i$ are slightly curved during the initial groups of the chain. This is reflected by a more pronounced initial increase in propagation speed (D), before it reaches

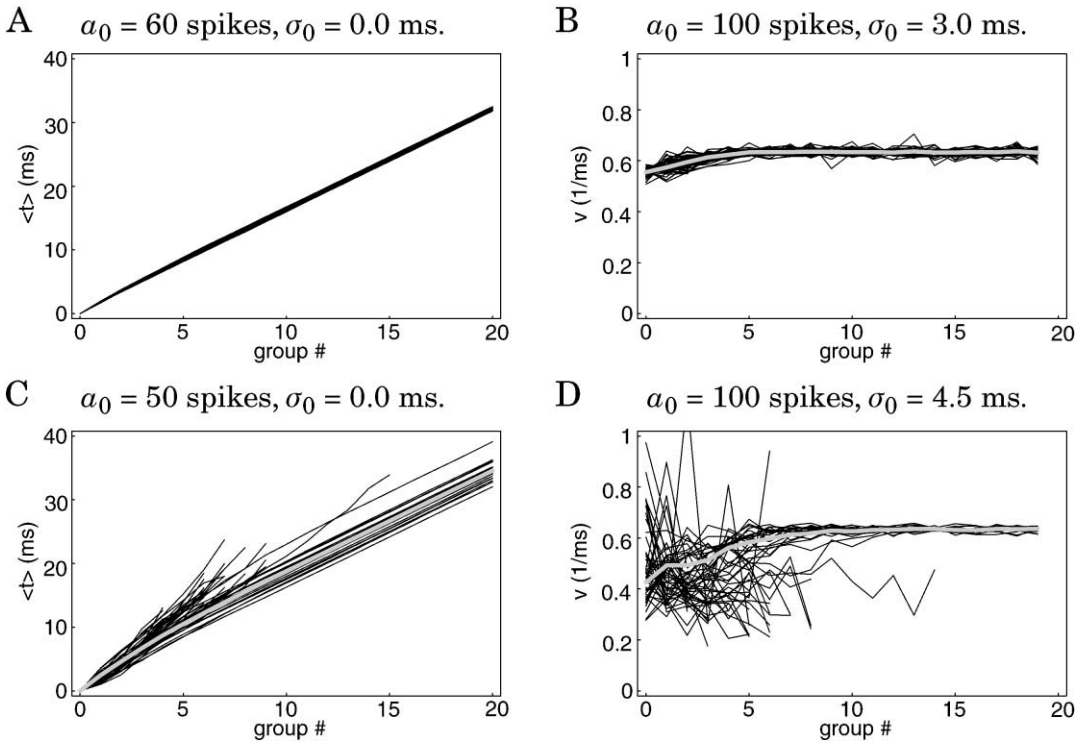

Fig. 8. Temporal mean of the pulse packet and the speed of propagation. (A) Temporal mean $\langle t \rangle$ versus group index. Same data as in Figs. 3A and 4A. The time at which the stimulus (specified in panel title) occurred is included at group number 0. Black lines correspond to individual trials, which merge at this resolution. Development is practically deterministic, and the delay between successive groups initially only slightly reduced. The average slope is ≈ 1.5 ms. (B) Propagation speed computed for the curves in A. The pulse packet first accelerates and reaches a saturating speed of ≈ 0.6 groups/ms. (C) Same graph as in A for the data in Figs. 3D and 4D. In the initial groups, successful and unsuccessful trials show large variability. Variability and delay between successive groups further increases for unsuccessful trials. For successful trials, variability practically drops to zero (delay as in A), leading to parallel curves (gray curve average of successful trials). (D) Same graph as in B for the data in C. Successful trials accelerate from an initial speed of ≈ 0.4 groups/ms to the same limiting value (0.6 groups/ms) as in B. Unsuccessful trials drop to a speed of about ≈ 0.4 groups/ms or even less.

the same constant value as in B. Moreover, the initial inter-trial variability in C is significantly larger than in A.

Inspecting the velocity curves (B and D), both the individual trials (black) and the averages over the surviving trials (gray), we note that as the pulse packet approaches the attractor, the propagation speed increases and the inter-trial variability decreases. Once the pulse packets become stable, they are not only faster, but their speed is also less variable, both across trials and across time within a trial. Initially, the velocity is clearly more variable, as can also be seen from the position plots (A and C), where the difference between individual trials first increases with group number, but later remains constant ('life-lines' become parallel). Note that in C the large variability of $\langle t \rangle$ at the end of the chain is only the result of the large initial variability in v, since beyond group number 10, v_i is practically constant across groups and across trials.

7. Discussion

7.1. Survival probability and state space

From our simulations, it appears that the propagation of volleys of synchronous spike activity through a chain of groups of neurons can be well described in the following way. A pulse packet is a set of spikes, distributed around a common temporal mean. The number of spikes a and their temporal dispersion (standard deviation) σ are the two main parameters of the pulse packet. A group of neurons receiving a pulse packet input modifies it according to its intrinsic transmission function. Typically, each neuron contributes not more than one spike to a pulse packet. The transformed pulse packet is then passed on to the neurons in the next group. This picture was already implicit during the discussion of Fig. 7, in that we assumed that the propagation can be uniquely described by the evolution of the pair (a, σ) along the chain.

Thus, each pulse packet propagation can be represented by a trajectory in the (a, σ)-space. Comparing individual trials, we observe a considerable variability across trials. Trajectories starting at different points in the state space cross due to this variability. Yet, near the attractor, the variability is considerably reduced. This allowed us to define and evaluate trial-averaged trajectories for different initial conditions. The averaged trajectories are much smoother and remain separated (within their error bounds).

Thus, we can interpret the *mean of the dynamics of pulse*

packet propagation, using the terminology of dynamical systems theory. In our previous paper (Diesmann et al., 1999), we described the *dynamics of the mean of pulse packet propagation*. There, the $a-\sigma$ state space showed a *separatrix*, which clearly separated the basin of attraction from the instable region (see also Câteau & Fukai, 2001, this volume; Gewaltig, 2000). In the state space shown here (cf. Fig. 7), the separatrix is replaced by a steep transition in the survival probability landscape.

The dynamic description treats the propagation of pulse packet activity as an iterative map. Such discrete systems may, in fact, show crossings of their state space trajectories. Yet, in Fig. 7, the averaged trajectories are clearly separated. Thus, at least in the region where we evaluated the trajectory averages, the description in terms of the two variables a and σ appears to be smooth. Note, however, that this only holds in the mean; in individual trials, the transition from one point in the state space to the next is non-deterministic, due to the background activity (cf. Figs. 5 and 6).

7.2. Sources of variability

The variability of a pulse packet depends on its position in state space. It is largest for small a and large σ, and smallest for large a and small σ. There are two possible sources for the observed variability: (1) a variability in the measured quantities a and σ, which is independent of the dynamics; and (2) a variability inherent to the system dynamics.

Estimation of the pulse packet activity a introduces variability, because we have to separate the spikes of a pulse packet from the background activity by some criterion (see the Appendix). For small a, the relative contribution of each spike to the estimated parameters is stronger than for large a and, thus, small errors in the separation process have a larger influence on the quality of the parameter estimation. Generally, our separation procedure (see the Appendix) systematically underestimates the value of a.

Since errors in the estimation of a directly affect the estimation of σ, this bias towards larger variability at smaller a causes a corresponding bias towards more variability in σ in low activity pulse packets. In addition, the estimation of σ operates on the distances of individual spike times from their mean. Thus, for low spike counts, single erroneous spikes at the border of a pulse packet have a particularly strong influence on the estimated σ-value.

Variability that is inherent to the system dynamics is introduced by the variability of the ongoing background input. If we assume that, in the mean, the firing behavior of a neuron is governed by a modulated Poisson process, then in each trial, the number of response spikes of a neuron group follows a Poisson distribution with the corresponding degree of variability. In each trial, the neurons receive a different number and constellation of input spikes from the preceding group.

Our earlier study (Diesmann et al., 1999) predicts that for smaller w, stable propagation of synfire activity is possible if the PSP amplitudes are upscaled accordingly. However, in narrower chains, the relative contribution of each spike is enhanced and, therefore, variability increases. The detailed investigation of such scaling behavior is the subject of ongoing work.

7.3. Stimulus coupling and background activity

In our simulations, the background activity in different neurons was considered mutually independent, stationary Poisson. It is known, however, that ongoing cortical activity exhibits coherent spatio-temporal structure (Arieli, Shoham, Hildesheim & Grinvald, 1995). Hence, neurons within a group that are anatomically close will tend to be excited (or inhibited) together by correlated background activity. Moreover, a strong relation has been found between ongoing network activity and the variability of evoked responses, both in single neurons and in population activity (Arieli et al., 1996b; Azouz & Gray, 1999; Tsodyks, Kenet, Grinvald & Arieli, 1999), as well as in behavioral responses (Arieli, Donchin, Aertsen, Bergmann, Gribova, Grinvald et al., 1996a). Clearly, both the spatio-temporal structure and the variability of the background activity should have a strong impact on the precise synchronization dynamics in pulse packet propagation and its time-locking to stimuli and behavioral events. The impact of such variable spatio-temporal coherence in background activity on the state space portrait of pulse packet transmission is the subject of current research (Mohns, Diesmann, Grün & Aertsen, 1999).

In Section 6.5 we demonstrated that the temporal coupling between stimulus packet and group response is practically identical throughout the chain. If the stimulus is weak, any relevant jitter is only accumulated during the first few groups, until the propagating pulse packet has gained and synchronized its activity. However, even in this case, the accumulated amount of jitter between stimulus and group response in a synfire chain with 100 neurons per group is not large enough to explain the loose stimulus coupling of experimentally observed firing patterns (Prut et al., 1998; Riehle et al., 1997). Thus, our results suggest that if the observed firing patterns are the result of synfire chains, activity propagation is not ignited by pulse packets. Rather, loose stimulus coupling could be the result of the transition from firing rates to synchronized activity: if the first few groups of a synfire chain experience a rate elevation of their input neurons, propagating pulse packets will be ignited in loose temporal relation to the onset of this rate elevation (Grün, 1996).

7.4. Membrane time constant

The temporal precision of the stable state, measured by the standard deviation of the associated spike time distribution, is in the sub-millisecond range. This means that essentially all response spikes in a volley fall within a window of 1–2 ms. This temporal precision is consistent with the high accuracy of experimentally observed spike patterns in cortical recordings, both in vivo (Abeles et al., 1993b; Prut et al.,

1998; Riehle et al., 1997) and in vitro (Mainen & Sejnowski, 1995; Nowak et al., 1997). Thus, in contrast to other model studies (Shadlen & Newsome, 1994, 1998), we conclude that highly precise synchronous firing of cortical neurons is indeed feasible, in spite of the large membrane time constant of 10 ms or more. In fact, the temporal precision of the spike response is not constrained by the membrane time constant itself; the limiting factor is the up-slope of the post-synaptic potential (PSP). The higher this slope, the faster the membrane potential response to a pulse packet traverses the threshold region (Abeles, 1991). This reduces the chance of interference with background fluctuations, which might reduce the timing precision of the response spike. However, the membrane time constant does limit the transmission of synchronous spikes, but rather in the opposite way. It determines the integration time window of the receiving neuron, thereby limiting the temporal extent over which a volley of incoming spikes is 'seen' as a single packet, rather than as isolated spikes. For too small a membrane time constant, the PSPs in response to a spike volley no longer overlap and, hence, cannot add up to reach threshold (Heck, Léger, Stern & Aertsen, 2000). Reliable transmission of incompletely synchronized spike volleys, therefore, requires a minimal (rather than a maximal) value of the membrane time constant, in the order of the duration of the volley.

7.5. Transmission delays and the precision of firing

The temporal precision of the stable state is not only determined by neuronal properties, such as the membrane time constant. It is also limited by the distribution of the transmission delays between neurons in successive groups. In our simulations, we assumed a uniform transmission delay of 1 ms for all inter-group connections, neglecting the fact that there will be a distribution of delays. Such a delay distribution introduces additional jitter at each stage in the synfire transmission and, thus, effectively de-synchronizes an emitted pulse packet on its way to the next group. This de-synchronization can be described by convolving (i.e. blurring) the output pulse packet of the sending group with the delay distribution of the inter-group connectivity. The result of this convolution then, in turn, serves as the input pulse packet for the receiving group. Effectively, this blurring amounts to a drift towards larger sigma at each stage of the trajectory in state space. The amount of this drift (i.e. the width of the delay distribution) determines the lower limit of the accuracy of pulse packet transmission. Moreover, it determines the size of the basin of attraction and the position of the separatrix. Thus, if the width of the delay distribution exceeds a critical value, trajectories may cross the separatrix (compared to the noiseless case and pulse packet propagation becomes unstable).

7.6. Learning of synfire chains

In a random network with moderate connectivity, many synfire chains can be found by chance (Abeles, 1991). For example, examine a random network that mimics a cortical hyper-column with 20,000 pyramidal neurons and a connectivity of 25%. If one selects a pool of 100 neurons by chance, there will almost always be another pool of 100 neurons in which every neuron is connected to at least 30 neurons from the first one. However, such random synfire chains may not function reproducibly, unless the synaptic connections are strengthened by some appropriate learning rule. It is not clear whether such learning can indeed happen spontaneously. Conflicting reports on this issue have appeared in the literature. Doursat (1993) claimed that this can be achieved easily. By contrast, Hertz and Prügel-Bennett (1996) had to carefully trim parameters to obtain self-organized synfire chains which, however, tended to fold upon themselves, forming short loops. Horn, Levy and Ruppin (2000) applied the time-asymmetric learning rule and obtained loops of 3–5 pools. They called activity in such a network distributed synchrony. Arndt, Aertsen and Abeles (1994) observed—both in simulations and by analytic calculations—that the velocity of synfire chain growth highly depends on the number of synchronously stimulated neurons and on the level of background activity. In all the networks above, there was no inhibition, thus, large pools with many neurons firing together could develop. Amit and Brunel (1997) and van Vreeswijk and Sompolinsky (1996, 1998) suggested a scenario of precise balance between excitation and inhibition that can maintain low average activity in a network.

7.7. Functional relevance of synfire chains

For each of the neurons in our network model, the roughly 100 synapses delivering spike activity from the preceding group and the additional 20,000 synapses delivering background activity were all taken as equally strong. The purpose was to find out whether stable transmission of synchronous spiking requires especially strong synapses between the neuron groups (either pre-wired or acquired by learning (Bienenstock, 1991, 1995; Herrmann, Hertz & Prügel-Bennett, 1995)). Our findings show that this is not the case: precisely synchronous activity can survive in the network without the need for dedicated strong synapses, provided that enough neurons can be recruited from group to group (note that neurons may participate in multiple groups if these are temporally separated by more than the neurons' refractory period: the network needs to be only *locally feed-forward*). From the receiving neuron's point of view, only the number of spikes arriving within a narrow (few ms) time window distinguishes the spikes in a pulse packet from other incoming activity. Thus, each neuron can potentially take part in a large number of synchronous processes with different neuron compositions, not limited by a fixed arrangement of synaptic weights. Moreover, a neuron that on one occasion takes part in the transmission of a synchronous spike volley, is considered as part of the background activity

on another. This arrangement allows for maximum flexibility in allocating neuronal resources by providing a substrate on which different configurations of synchronous activity can flourish and develop meaningful associations among neurons. This enables the network to dynamically configure itself into functional groupings, depending on the instantaneous computational demands. Combined with a certain degree of randomness in the local connectivity (Hellwig, 2000; Hellwig, Schüz & Aertsen, 1994), it imposes minimal structural constraints on which neural associations may eventually evolve, utilizing all degrees of freedom afforded by the available synaptic connectivity.

8. Summary and conclusions

Taken together, the results of our network simulations of synfire activity correspond well to our earlier predictions, based on single neuron properties (Diesmann et al., 1999). For sufficiently large groups ($w > 100$ neurons), we observe stable propagation of synfire activity. This propagation can be fully described by just two parameters, the number of spikes a in volley and their temporal jitter σ. There exists a wide range of stimulus parameters for which the pulse packet is likely to evolve towards a stable attractor. Within the basin of attraction, the survival probability is close to one; outside it, the survival probability rapidly drops to zero. Moreover, the location of this transition matches the separatrix in our state space description (Diesmann et al., 1999; Gewaltig, 2000). Taken together, our findings indicate that the accuracy of activity propagation in the cortical network is precise and robust enough to explain the precision (~1 ms) of experimentally observed spike patterns (Abeles et al., 1993a; Riehle et al., 1997).

Acknowledgements

Stimulating discussions with Moshe Abeles, Elie Bienenstock, and Stefan Rotter are gratefully acknowledged. Partial funding was received from the Deutsche Forschungsgemeinschaft (DFG), the Human Frontier Science Program (HFSP) and the German–Israeli Foundation for Research and Development (GIF).

Appendix A. Estimation of pulse packet parameters

For each choice of stimulus parameters (a_0, σ_0), we obtain a data file that contains the activity of all neurons in the chain for all N trials ($N = 50$). We process the spike trains of each group separately. Within each spike train we search for the propagating pulse packet.

Since the data are noisy, due to the background activity, the spikes of a possibly present pulse packet will be embedded in spontaneous events. We use knowledge about the strength of spontaneous activity in order to separate the pulse packet response from the 'noise' background. In the first step, we reduce the spike train to a region of interest by applying a noise threshold to the event density. In a second step, we remove all isolated events, i.e. they are considered spontaneous.

The 'region of interest' is determined by searching for the highest event density within the spike train, and selecting a certain region around the time of the highest event density. To this end, the event density is estimated using a PST histogram with 5 ms bin size.

A threshold θ_n is used to distinguish between a low density spontaneous event cluster and a pulse packet. The threshold value θ_n is chosen by estimating the expected number of spontaneous events within a bin of the histogram.

Assuming the spontaneous events obey a Poisson distribution (we actually tested this for a number of cases and found this property to be approximated quite well) with a rate $\lambda = 2/\text{s}$ per neuron, the expected number of events in an interval $\Delta = 5$ ms is given by:

$$\langle n \rangle = w\lambda\Delta$$

$$= 100 \cdot 2 \times 10^{-3}\ \text{ms}^{-1} \cdot 5\ \text{ms}$$

$$= 1.$$

The threshold θ_n is chosen well above this value at $\theta_n = 10$.

The next processing step tries to remove those spontaneous events which do not directly coincide with the pulse packet. Thus, we remove all events from the data which appear isolated within a certain time interval t_θ. An event t_j was removed if

$$|t_{j-1} - t_j| > t_\theta \text{ or } |t_{j+1} - t_j| > t_\theta.$$

Choosing t_θ too small will lose events at the borders of the pulse packet, choosing it too large will leave too much noise in the data. We found that a value of t_θ between 0.3 and 2.0 ms results in a good compromise between these two extremes.

We define the remaining events as the *pulse packet*. The number of events a is called the *activity of the packet*. If there are no more events left in the train, i.e. $a = 0$, we conclude that the previous group was not strong enough to trigger a pulse packet response of this synfire group.

The mean and standard deviation of a pulse packet are estimated according to the formulae:

$$\langle t \rangle = \frac{1}{a} \sum_{j=1}^{a} t_j \tag{20}$$

$$\sigma^2 = \frac{1}{a} \sum_{j=1}^{a} (\langle t \rangle - t_j)^2 \tag{21}$$

All analysis was done using the *Mathematica* system (Wolfram, 1996).

References

Abeles, M. (1982). *Local cortical circuits: an electrophysiological study*, Berlin, Heidelberg, New York: Springer-Verlag.

Abeles, M. (1982b). Role of cortical neuron: integrator or coincidence detector? *Israel Journal of Medical Sciences*, *18*, 83–92.

Abeles, M. (1991). *Corticonics: neural circuits of the cerebral cortex*, Cambridge: Cambridge University Press.

Abeles, M., Bergman, H., Margalit, E., & Vaadia, E. (1993a). Spatiotemporal firing patterns in the frontal cortex of behaving monkeys. *Journal of Neurophysiology*, *70*, 1629–1638.

Abeles, M., Vaadia, E., Prut, Y., Haalman, I., & Slovin, H. (1993b). Dynamics of neuronal interactions in the frontal cortex of behaving monkeys. *Concepts in Neuroscience*, *4*, 131–158.

Aertsen, A., & Arndt, M. (1993). Response synchronization in the visual cortex. *Current Opinion in Neurobiology*, *3*, 586–594.

Aertsen, A., Diesmann, M., & Gewaltig, M.-O. (1996). Propagation of synchronous spiking activity in feedforward neural networks. *Journal of Physiology (Paris)*, *90*, 243–247.

Aertsen, A., Vaadia, E., Abeles, M., Ahissar, E., Bergman, H., Karmon, B., Lavner, Y., Margalit, E., Nelken, I., & Rotter, S. (1991). Neural interactions in the frontal cortex of a behaving monkey: signs of dependence on stimulus context and behavioral state. *Journal für Hirnforschung*, *32*, 735–743.

Ahissar, M., Bergman, E. A., & Vaadia, E. (1992). Encoding of sound-source location and movement: activity of single neurons and interactions between adjacent neurons in the monkey auditory cortex. *Journal of Neurophysiology*, *67*, 203–215.

Amit, D. J., & Brunel, N. (1997). Model of global spontaneous activity and local structured activity during delay periods in the cerebral cortex. *Cerebral Cortex*, *7*, 237–252.

Arieli, A., Donchin, O., Aertsen, A., Bergmann, H., Gribova, A., Grinvald, A., & Vaadia, E. (1996a). The impact of ongoing cortical activity on evoked potentials and behavioral responses in the awake behaving monkey. *Society for Neuroscience Abstracts*, *22*, 2022.

Arieli, A., Shoham, D., Hildesheim, R., & Grinvald, A. (1995). Coherent spatiotemporal patterns of ongoing activity revealed by real-time optical imaging coupled with single-unit recording in the cat visual cortex. *Journal of Neurophysiology*, *73*, 2072–2093.

Arieli, A., Sterkin, A., Grinvald, A., & Aertsen, A. (1996b). Dynamics of ongoing activity: explanation of the large variability in evoked cortical responses. *Science*, *273*, 1868–1871.

Arndt, M., Aertsen, A., & Abeles, M. (1994). The potential functional role of reverberating synfire chains developing in randomly connected neural networks. *Society for Neuroscience Abstracts*, 1395.

Azouz, R., & Gray, C. M. (1999). Cellular mechanisms contributing to response variability of cortical neurons in vivo. *Journal of Neuroscience*, *19*, 2209–2223.

Barlow, H. B. (1972). Single units and sensation: a neuron doctrine for perceptual psychology? *Perception*, *1*, 371–394.

Barlow, H. (1992). Single cells versus neuronal assemblies. In A. Aertsen & V. Braitenberg, *Information processing in the cortex* (pp. 167–173). Berlin, Heidelberg, New York: Springer-Verlag.

Bi, G., & Poo, M. (1998). Synaptic modification in cultured hippocampal neurons: dependence on spike timing, synaptic strength, and postsynaptic cell type. *Journal of Neuroscience*, *18*, 10464–10472.

Bienenstock, E. (1991). Notes on the growth of a 'composition machine'. In D. Andler, E. Bienenstock & B. Laks, *Contributions to Interdisciplinary Workshop on Compositionality in Cognition and Neural Models* (pp. 1–19). Asniere s. Oise, France: Abbaye de Royaumont.

Bienenstock, E. (1995). A model of neocortex. *Network: Computation in Neural Systems*, *6*, 179–224.

Boven, K.-H., & Aertsen, A. (1990). Dynamics of activity in neuronal networks give rise to fast modulations of functional connectivity. In R. Eckmiller, G. Hartmann & G. Hauske, *Parallel processing in neural systems and computers* (pp. 53–56). Amsterdam: Elsevier.

Braitenberg, V., & Schüz, A. (1991). *Anatomy of the cortex: statistics and geometry*. Berlin, Heidelberg, New York: Springer-Verlag.

Calvin, W. H., & Stevens, C. F. (1968). Synaptic noise and other sources of randomness in motoneuron interspike intervals. *Journal of Neurophysiology*, *31*, 574–587.

Câteau, H., & Fukai, T. (2001). Fokker–Planck approach to pulse packet propagation in synfire chain. *Neural Networks*, *14* (this issue).

De Charms, R. C., & Merzenich, M. (1995). Primary cortical representation by the coordination of action potential timing. *Nature*, *381*, 610–613.

Diesmann, M., Gewaltig, M.-O., & Aertsen, A. (1996). Characterization of synfire activity by propagating 'pulse packets'. In J. M. Bower, *Computational neuroscience: trends in research* (pp. 59–64). San Diego: Academic Press.

Diesmann, M., Gewaltig, M.-O., & Aertsen, A. (1999). Stable propagation of synchronous spiking in cortical neural networks. *Nature*, *402*, 529–533.

Diesmann, M., Gewaltig, M.-O., & Rotter, S., & Aertsen, A. (2001). State space analysis of synchronous spiking in cortical networks. *Neurocomputing*, *38–40*, 565–571.

Doursat, R. (1993). *Contribution a l'etude des representations dans le systeme nerveux et dans les reseaux de neurones formels*. Unpublished doctoral dissertation, University of Paris IV.

Eckhorn, R., Bauer, R., Jordan, W., Brosch, M., Kruse, W., Munk, M., & Reitböck, H. J. (1988). Coherent oscillations: a mechanism of feature linking in the visual cortex? *Biological Cybernetics*, *60*, 121–130.

Eggermont, J. J. (1992). Neural interaction in cat primary auditory cortex II. Effects of sound stimulation. *Journal of Neurophysiology*, *71*, 246–270.

Engel, A. K., König, P., Schillen, T. B., & Singer, W. (1992). Temporal coding in the visual cortex: new vistas on integration in the nervous system. *Trends in Neurosciences*, *15*, 218–226.

Fetz, E. (1997). Temporal coding in neural populations? *Science*, *278*, 1901–1902.

Fetz, E., Toyama, K., & Smith, W. (1992). Synaptic interactions between cortical neurons. In A. Peters, *Cerebral cortex* (pp. 1–47), vol. 9. New York: Plenum Publishing Corporation.

Georgopoulos, A. P., Tiara, M., & Lukashin, A. (1993). Cognitive neurophysiology of the motor cortex. *Science*, *260*, 47–52.

Gerstein, G. L., Bedenbaugh, P., & Aertsen, A. (1989). Neuronal assemblies. *IEEE Transactions on Biomedical Engineering*, *36*, 4–14.

Gerstner, W., Kempter, R., van Hemmen, J. L., & Wagner, H. (1996). A neuronal learning rule for sub-millisecond temporal coding. *Nature*, *383*, 76–78.

Gewaltig, M.-O. (2000). (PhD thesis). *Evolution of synchronous spike volleys in cortical networks—network simulations and continuous probabilistic models*, Aachen, Germany: Shaker Verlag.

Gewaltig, M.-O., Diesmann, M., & Aertsen, A. (1995). Role of the cortical neuron: both integrator and coincidence detector. In R. Menzel & N. Elsner, *Learning and Memory: Proceedings of the 23rd Göttingen Neurobiology Conference* (p. 555), vol. 2. Stuttgart, New York: Thieme.

Gewaltig, M.-O., Diesmann, M., & Aertsen, A. (2001). Cortical synfire-activity: configuration space and survival probability. *Neurocomputing*, 38–40, 621–626.

Gewaltig, M. -O., Diesmann, M., Aertsen, A., & Abeles, M. (1994). A realistic and computationally efficient model of cortical pyramidal neurons. In N. Elsner & H. Breer, *Proceedings of the 23rd Göttingen Neurobiology Conference* (p. 559), vol. 2. Stuttgart, New York: Thieme.

Gray, C. M., & Singer, W. (1989). Stimulus-specific neuronal oscillations in orientation columns of cat visual cortex. *Proceedings of the National Academy of Sciences USA*, *86*, 1698–1702.

Griffith, J. S. (1963). On the stability of brain-like structures. *Biophysical Journal*, *3*, 299–308.

Grün, S. (1996). *Unitary joint-events in multiple-neuron spiking activity: detection, significance, and interpretation*, Thun, Frankfurt/Main: Verlag Harri Deutsch.

Gütig, R., Aharonov-Barki, R., Rotter, S., Aertsen, A., & Sompolinsky, H.

(2001). Generalized synaptic updating in temporally Hebbian learning. In *Neurobiology Report 2001. Proceedings of the 28th Göttingen Neurobiology Conference*. Stuttgart, Germany: Thieme (in press).

Hebb, D. O. (1949). *Organization of behavior: a neuropsychological theory*, New York: John Wiley & Sons.

Heck, D., Léger, J. F., Stern, E. A., & Aertsen, A. (2000). Size and summation of synchronous and asynchronous population PSPs in rat neocortical neurons: intracellular recordings in vivo with dual intracortical microstimulation. *Society for Neuroscience Abstracts*, *26*, 1623.

Hehl, U., Hellwig, B., Rotter, S., Diesmann, M., & Aertsen, A. (2001). Anatomical constraints on stable propagation of synchronous spiking in cortical networks. In *Neurobiology Report 2001. Proceedings of the 28th Göttingen Neurobiology Conference*. Stuttgart, Germany: Thieme (in press).

Hellwig, B. (2000). A quantitative analysis of the local connectivity between pyramidal neurons in layers 2/3 of the rat visual cortex. *Biological Cybernetics*, *82*, 111–121.

Hellwig, B., Schüz, A., & Aertsen, A. (1994). Synpases on axon collaterals of pyramidal cells are spaced at random intervals: a Golgi study in the mouse cerebral cortex. *Biological Cybernetics*, *71*, 1–12.

Herrmann, M., Hertz, J. A., & Prügel-Bennett, A. (1995). Analysis of synfire chains. *Network: Computation in Neural Systems*, *6*, 403–414.

Hertz, J., & Prügel-Bennett, A. (1996). Learning short synfire chains by self-organization. *Network*, *7*, 357–363.

Horn, D., Levy, N., & Ruppin, E. (2000). Distributed synchrony of spiking neurons *Neurocomputing*, (32–33) 409–414.

Hubel, H. D., & Wiesel, T. N. (1977). Functional architecture of macaque monkey visual cortex. *Proceedings of the Royal Society London*, *198*, 1–59.

Jack, J. J. B., Noble, D., & Tsien, R. W. (1985). *Electric current flow in excitable cells*, Oxford: Clarendon.

Johannesma, P., Aertsen, A., van den Boogaard, H., Eggermont, J., & Epping, W. (1986). From synchrony to harmony: ideas on the function of neural assemblies and on the interpretation of neural synchrony. In G. Palm & A. Aertsen, *Brain theory* (pp. 25–47). Berlin: Springer-Verlag.

Kandel, E. R., Schwartz, J. H., & Jessel, T. M. (1991). *Principles of neural science*, (3rd ed). New York: Elsevier.

Lapicque, L. (1907). Recherches quantitatives sur l'excitation electrique des nerfs traitee comme une polarization. *Journal de Physiologie et de Pathologie générale*, *9*, 620–635.

Mainen, Z. F., & Sejnowski, T. J. (1995). Reliability of spike timing in neocortical neurons. *Science*, *268*, 1503–1506.

Markram, H., Lübke, J., Frotscher, M., & Sakmann, B. (1997). Regulation of synaptic efficacy by coincidence of postsynaptic APs and EPSPs. *Science*, *275*, 213–215.

Mohns, M., Diesmann, M., Grün, S., & Aertsen, A. (1999). Interaction of synchronous input activity and subthreshold oscillations of membrane potential. In *Neurobiology Report 1999. Proceedings of the 27th Göttingen Neurobiology Conference*. Stuttgart, Germany: Thieme.

Murthy, V. N., & Fetz, E. E. (1992). Coherent 25- to 35-Hz oscillations in the sensorimotor cortex of awake behaving monkeys. *Proceedings of the National Academy of Sciences USA*, *89*, 5670–5674.

Newsome, W. T., Britten, K. H., & Movshon, J. A. (1989). Neuronal correlates of a perceptual decision. *Nature*, *341*, 52–54.

Nicolelis, M. A. L., Baccala, L. A., Lin, R. C. S., & Chapin, J. K. (1995). Sensorimotor encoding by synchronous neural assembly activity at multiple levels in the somatosensory system. *Science*, *268*, 1353–1358.

Nowak, L. G., Sanchez-Vives, M. V., & McCormick, D. A. (1997). Influence of low and high frequency inputs on spike timing in visual cortical neurons. *Cerebral Cortex*, *7*, 487–501.

Palm, G. (1990). Cell assemblies as a guideline for brain research. *Concepts in Neuroscience*, *1*, 133–147.

Perkel, D. J., & Bullock, T. H. (1968). Neural coding. *Neuroscience Research Progress Bulletin*, *6*, 221–348.

Prut, Y., Vaadia, E., Bergman, H., Haalman, I., Slovin, H., & Abeles, M. (1998). Spatiotemporal structure of cortical activity: properties and behavioral relevance. *Journal of Neurophysiology*, *79*, 2857–2874.

Riehle, A., Grün, S., Diesmann, M., & Aertsen, A. (1997). Spike synchronization and rate modulation differentially involved in motor cortical function. *Science*, *278*, 1950–1953.

Roelfsema, P. R., Engel, A. K., König, P., & Singer, W. (1996). The role of neuronal synchronization in response selection: a biologically plausible theory of structured representations in the visual cortex. *Journal of Cognitive Neuroscience*, *8*, 610–613.

Rubin, J., Lee, D., & Sompolinsky, H. (2001). Equilibrium properties of temporally asymmetric Hebbian plasticity. *Physical Review Letters*, *86*, 364–367.

Sakurai, Y. (1996). Population coding by cell assemblies—what it really is in the brain. *Neuroscience Research*, *26*, 1–16.

Sanes, J. N., & Donoghue, J. P. (1993). Oscillations in local field potentials of the primate motor cortex during voluntary movement. *Proceedings of the National Academy of Sciences USA*, *90*, 4470–4474.

Shadlen, M. N., & Newsome, W. T. (1994). Noise, neural codes and cortical organization. *Current Opinion in Neurobiology*, *4*, 569–579.

Shadlen, M. N., & Newsome, W. T. (1998). The variable discharge of cortical neurons: implications for connectivity, computation, and information coding. *Journal of Neuroscience*, *18*, 3870–3896.

Singer, W. (1993). Synchronization of cortical activity and its putative role in information processing and learning. *Annual Review in Physiology*, *55*, 349–374.

Singer, W., & Gray, C. M. (1995). Visual feature integration and the temporal correlation hypothesis. *Annual Review in Neuroscience*, *18*, 555–586.

Softky, W. R., & Koch, C. (1993). The highly irregular firing of cortical cells is inconsistent with temporal integration of random EPSPs. *Journal of Neuroscience*, *13*, 334–350.

Song, S., Miller, K. D., & Abbot, L. F. (2000). Competitive Hebbian learning through spike-time-dependent synaptic plasticity. *Nature Neuroscience*, *3*, 919–926.

Stevens, C. F., & Zador, A. M. (1998). Input synchrony and the irregular firing of cortical neurons. *Nature Neuroscience*, *1*, 210–217.

Tsodyks, M., Kenet, T., Grinvald, A., & Arieli, A. (1999). Linking spontaneous activity of single cortical neurons and the underlying functional architecture. *Science*, *286*, 1943–1946.

Tuckwell, H. C. (1988). *Introduction to theoretical neurobiology*, Cambridge: Cambridge University Press.

Vaadia, E., Haalman, I., Abeles, M., Bergman, H., Prut, Y., Slovin, H., & Aertsen, A. (1995). Dynamics of neuronal interactions in monkey cortex in relation to behavioural events. *Nature*, *373*, 515–518.

Volgushev, M., Christakova, M., & Singer, W. (1998). Modification of discharge patterns of neocortical neurons by induced oscillations of the membrane potential. *Neuroscience*, *83*, 15–25.

von der Malsburg, C. (1981). *The correlation theory of brain function* (Internal report 81-2). Göttingen, FRG: Max-Planck-Institute for Biophysical Chemistry.

van Vreeswijk, C., & Sompolinsky, H. (1996). Chaos in neuronal networks with balanced excitatory and inhibitory activity. *Science*, *274*, 1724–1726.

van Vreeswijk, C., & Sompolinsky, H. (1998). Chaotic balanced state in a model of cortical circuits. *Neural Computation*, *10*, 1321–1371.

Wennekers, T., & Palm, G. (1996). Controlling the speed of synfire chains. In *Proceedings of the International Conference on Artificial Neural Networks ICANN '96* (pp. 451–456). Berlin: Springer.

Wolfram, S. (1996). *The Mathematica book*, (3rd ed). Cambridge, UK: Wolfram Media/Cambridge University Press.